NRCC
NATIONAL RESOURCE FOR COMPUTATION IN CHEMISTRY

Submitted to Chemical Physics

ROTATIONAL EXCITATION OF CO BY He IMPACT

L. D. Thomas, W. P. Kraemer and G. H. F. Diercksen

March 1980

TWO-WEEK LOAN COPY

This is a Library Circulating Copy
which may be borrowed for two weeks.
For a personal retention copy, call
Tech. Info. Division, Ext. 6782.

LAWRENCE BERKELEY LABORATORY
UNIVERSITY OF CALIFORNIA

DISCLAIMER

ROTATIONAL EXCITATION OF CO BY He IMPACT

L. D. Thomas,[*] W. P. Kraemer and G. H. F. Diercksen

Max-Planck-Institut für Physik und Astrophysik
8046 Garching bei München, West Germany

ABSTRACT

To study rotational excitations of CO by He impact, configuration-interaction potential energy surfaces have been computed with two different basis sets. The surfaces are compared to one another, to an electron-gas surface, and to an experimentally determined surface. In addition, converged close-coupling calculations of the collision cross sections have been done on these surfaces for energies up to 100 cm^{-1} and compared. On the most accurate CI surface, cross sections have been computed using the infinite-order sudden (IOS) and quasi-classical methods as well.

[*]Present address: National Resource for Computation in Chemistry,
Lawrence Berkeley Laboratory, University of California, Berkeley, CA 94720.

1. INTRODUCTION

Dense interstellar molecular clouds [1] are chiefly composed of molecular hydrogen. However, since H_2 in these clouds has no observable spectrum and is not excited by thermal collisions, trace constituents play fundamental roles in observations and in the understanding of the thermal balance of these clouds. The CO molecule has been found to be one of the most prevalent trace constituents in the dense clouds. It has observable dipole-allowed transitions and a small rotational constant so that it can be rotationally excited by low-temperature, thermal collisions. For these reasons, collisions of CO with the most abundant species, such as H_2, H, H^+ and He, have recently been receiving much experimental and theoretical attention.

The interaction between CO and He is the easiest of the four to study theoretically because the two collision partners are closed-shell systems in their electronic ground states, and the interaction between them is of short-range character. Further advantages from the computational point of view for systems like CO/He are that they have rather few nuclear degrees of freedom (i.e., the dimension of the interaction potential hypersurface is small) and the total number of electrons in the system is small enough to make feasible accurate quantum-chemical calculations of the interaction potential. We have therefore chosen the CO/He system as a test case to study the sensitivity of the collision cross sections to the accuracy of the theoretically computed interaction potential and to the level of approximation used in the dynamical calculations.

2.   DETERMINATION OF INTERACTION POTENTIAL HYPERSURFACES

Two different contracted Gaussian-type basis sets were used to approximate the molecular orbitals in the SCF calculations: (i) a "double-zeta" quality basis set plus polarization functions on each nuclear center, and (ii) a "triple-zeta" quality set plus an enlarged set of polarization functions. The first, called the "standard" or DZ-set in the following discussion, is known to produce reliable internal molecular geometries and quite accurate total electronic energies [2]. The second basis set, referred to here as the "extended" or TZ-set, was designed to reduce the so-called basis set superposition error in the interaction potential between CO and He and to describe particularly the He atom polarizability accurately [3]. For both basis sets the CO/He interaction potential hypersurfaces were determined separately in order to study directly the basis set dependence of the scattering results.

SCF calculations are known to cover only the electrostatic, induction and charge transfer effects which can be expected to be of minor importance here. The main contribution to the weak interaction between CO and He is, however, due to dispersion forces. Therefore, inclusion of electron correlation by configuration interaction (CI) calculations is essential for describing the CO/He interaction. In the CI calculations all single and double replacements from the Hartree-Fock closed shell single determinant reference configuration were taken into account (CISD). In addition, the contributions of certain quadruple excitations were estimated using the simple semi-empirical Davidson formula (CISDQ).

The potential hypersurfaces were computed pointwise for seven different orientation angles θ between the CO bond axis and the vector pointing from

the center of mass of CO to the helium atom and for each θ for about ten

different R values, where R is the distance between He and the CO

center of mass. For all these points the CO bond length was kept fixed

at its experimental value of r(CO) = 1.128 Å. In the context of the

astrophysical interest in this process this rigid rotor approximation

is well justified because collisional energies in the dense interstellar

clouds are small compared to the vibrational energy level spacings of CO.

More details about the quantum-chemical *ab initio* calculations of

the CO/He interaction potential hypersurfaces and a discussion of the

accuracy problems will be published elsewhere [4].

3. COMPARISON OF THE POTENTIAL HYPERSURFACES AND
   THEIR ANALYTIC FITS

With the notations defined earlier, we will compare five different

potential hypersurfaces:

(i) DZ-SCF, the SCF surface from the standard basis set calculations;

(ii) DZ-CISD, the CI surface, based on the standard basis set,
     including all single and double excitations;

(iii) DZ-CISDQ, the standard basis set CISD surface plus the
      Davidson correction for certain quadruple excitations;

(iv) TZ-CISDQ, the extended basis set CISD surface plus the
     Davidson correction; and

(v) GT, the electron-gas surface of Green and Thaddeus [5].

The *ab initio* calculated interaction potential values $V(R,\theta)$ of the surfaces

(i)-(iv) are listed in table 1, where $V(R,\theta)$ is obtained as the difference

between the actual energy values $E(R,\theta)$ and the energy of the non-inter-

action subsystems E_∞.

Analytic fits to these surfaces were made in the usual way. They were first expanded in Legendre polynomials:

$$V(R,\theta) = \sum_\lambda V_\lambda(R) \, P_\lambda(\cos\theta) \tag{1}$$

and the radial coefficients V_λ were then fit to the form

$$V_\lambda(R) = \sum_i a_i \, e^{-b_i R} + \sum_j c_j R^{-m_j} \; . \tag{2}$$

The parameters for the fits are given in table 2.

The asymptotic forms for the radial coefficients V_λ are given by Chu and Dalgarno [6]. For the first four terms these are:

$$V_0(R) = -9.005 \, R^{-6} \tag{3}$$

$$V_1(R) = -5.501 \, R^{-7} \tag{4}$$

$$V_2(R) = -1.503 \, R^{-6} \tag{5}$$

$$V_3(R) = -1.424 \, R^{-7} \tag{6}$$

where the following values (in atomic units) for the atomic and molecular properties were used:

$$\alpha \text{ (He)} = 1.39 \qquad [7]$$

$$U \text{ (He)} = 0.9036 \qquad [8]$$

$$\alpha_\parallel \text{ (CO)} = 17.54 \qquad [9]$$

$$\alpha_\perp \text{ (CO)} = 10.96 \qquad [9]$$

$$U \text{ (CO)} = 0.5150 \qquad [10]$$

$$\mu \text{ (CO)} = -0.0441 \qquad [11]$$

$$Q \text{ (CO)} = -1.8587 \qquad [12]$$

The TZ-CISDQ surface does have the proper limiting form for the V_0 and V_2 terms, but only at R-values where the potential is already very small. For this reason, the $c_j R^{-m_j}$ terms in eq. (2) were not very helpful for fitting. In most cases, using them made good fits more difficult to obtain, and even when they were used, the coefficients c_j turned out to be not physically meaningful. This is in contrast to the CO/Li$^+$ system where the identical fitting procedure yielded good values for the c_j coefficients [13].

The relative percent errors for the TZ-CISDQ surface are shown in table 3. The fits for the other surfaces of this study are of similar accuracy. Due to the extreme shallowness of the wells, these fits do not have as high a relative accuracy as do fits for the CO/Li$^+$ surfaces using this same technique [13,14], although the absolute errors are no larger.

The V_λ terms of the different theoretical potentials are shown in fig. 1. Comparing the DZ-CISDQ and the TZ-COSDQ V_λ terms shows a general lowering of the interaction potential hypersurface with increasing basis set size, as is to be expected, and a decreasing value for the location of the minimum, R_m. The most obvious difference from the GT surface is the well depth. This was adjusted by Green and Thaddeus [5] so that the well depth of the V_0 term agreed with values which have been inferred from experimental data.

In fig. 2, the V_0 terms are compared to the inferred potential from a more recent experiment [15] which lies about halfway between the GT and TZ-CISDQ surfaces. Comparison of the TZ- and DZ-CISDQ V_0 terms shows that increasing the basis set size does shift the theoretical potential in the direction of the experimental potentials. However, due to the discrepancies

between experiments and to the ambiguous nature of inferring a potential

from experimental data, it is not possible at the moment to say which

of these surfaces is more nearly correct.

The differences between the CI and the GT surfaces in the well region

are even more exaggerated in the anisotropic terms, $\lambda > 0$. It is therefore

expected that the orbiting resonance structure in the cross sections at

low energy will be quite different for the SCF, the various CI, and the

GT surfaces. The irregularities due to the interpolation procedure of

Green and Thaddeus are not expected to have a significant effect on the

quantum scattering.

It is also apparent that the GT surface is contracted by 1-2 bohr

compared to the CI surfaces. On the GT surface the incoming He atom thus

sees a smaller target with a much more attractive potential well. There-

fore, it would be expected that the scattering cross sections would be

significantly different.

The only respect in which the GT surface is similar to the others

is that the angular dependence in the repulsive wall region is qualitatively

the same, but even then only when scaled radially. This is illustrated in

fig. 3. This figure shows $V(r=5.0,\theta)$ for the TZ-CISDQ, DZ-CISDQ, DZ-CISD

and DZ-SCF surfaces and $V(R=4.67,\theta)$ for the GT surface.

As mentioned before, one surprising feature of the CI surfaces is

their asymptotic behavior at large R. At first they appeared not to have

the behavior predicted by perturbation theory [16]. After reducing the

size of the convergence criterion in the diagonalization, sufficient

accuracy was achieved at R = 10, 11 and 12 bohr to establish that the

calculations did in fact yield the proper behavior. In the case of the

extended basis set, even the values for the coefficients of the inverse
powers of R were in good agreement with perturbation theory. This is
shown in fig. 4. However, by the time this asymptotic behavior is reached,
the potential energy is already so small that its influence on the
scattering is small.

4.   CROSS SECTIONS AND COMPARISONS

Cross sections have been computed for collision energies up to 100
cm^{-1}. Close coupling calculations have been done for the DZ-SCF, DZ-CISDQ
and TZ-CISDQ surfaces, using the same computer programs and basis sets
as Green and Thaddeus [5]. These results are compared in fig. 5. In
addition, cross section calculations have been done for the TZ-CISDQ
surface using the infinite-order sudden (IOS) approximation [17] and the
quasiclassical (QC) method [18]. These results are shown in fig. 6.

The close coupling calculations allow us to compare the cross
sections for several levels of accuracy in the potential energy surface
while holding the dynamical approximation fixed. The IOS and QC
calculations allow us to compare different levels of accuracy in the
dynamical approximations while holding the potential energy surface
fixed.

The CISD and CISDQ surfaces are so similar, especially for $\lambda > 0$,
that separate scattering calculations were not done for them. The CISDQ
is assumed to be the more accurate of the two.

Comparing the DZ-SCF and DZ-CISDQ results shows the sensitivity of
the cross sections to the effects of configuration interaction. The
largest difference is in the low-energy, resonance region. Since the

DZ-CISCF surface had hardly any attractive well, the cross sections
for this surface show almost no resonance structure. As the energy
increases, the difference between the cross sections for these two
surfaces decreases. The differences at 100 cm^{-1} are in the range 10-35%.

Comparing the cross sections for the DZ-CISDQ and the TZ-CISDQ shows
the effect of increasing the basis set size while holding the *level* of
the CI calculation fixed. These cross sections show similar resonance
structures and qualitatively the same energy dependencies. Differences
range from about 1% for the $0 \rightarrow 0$ transition to about 30% for the $0 \rightarrow 4$
transition.

Finally we compare the cross sections from the electron gas surface (GT)
and the TZ-CISDQ surface. These represent, respectively, the simplest and
most difficult *ab initio* surfaces which can currently be computed for this
system. The cross sections are qualitatively similar in the inelastic
but different in the elastic transitions. The differences are in the range
30-50% in the odd transition and 100-200% in the even transitions. We
also note that the differences are positive for the even transitions and
negative for the odd.

In order to compare the sensitivity of the cross sections to the
dynamical approximations, IOS and QC calculations were also done for the
TZ-CISDQ surface. These are compared to the close coupling cross sections
in fig. 6. Neither the IOS nor the QC method is expected to be accurate
near the threshold or in the resonance region.   Above those
regions they do quite well. The IOS method in particular does remarkably
well for the $0 \rightarrow 0$ and $0 \rightarrow 1$ transitions. Its accuracy begins to deteriorate,
however, as the transitions approach the upper allowed limit.

A comparison of all cross sections for transitions $0 \rightarrow j'$, $j' = 0,1,2,3,4$ is given in table 4. Since the close-coupling cross sections for the TZ-CISDQ surface are the most accurate calculations done for this system to date, all others are compared as percent difference from them. The values in table 4 were computed from $100 (\sigma - \sigma')/\sigma'$, where σ' is the corresponding cross section for the TZ-CISDQ surface.

5. SUMMARY

We have computed SCF and CI potential energy surfaces for He-CO with two different basis sets. These surfaces have been compared to an electron gas surface and to a spherically averaged surface, inferred from experimental data. The electron gas surface is found to have an attractive well which is about twice as deep and contracted by about 1 bohr compared to the best CI surface. The experimental surface has a well depth about 1.5 times as deep as the best CI surface. Improving the quality of the computed surface by increasing both the level of the CI calculation and the size of the orbital basis set changes the potential in the direction of the experimental surface.

Scattering cross sections have been computed for collision energies up to 100 cm^{-1} using the close coupling, IOS and quasiclassical (QC) methods. Below 50 cm^{-1} the scattering cross sections are dominated by orbiting resonances and are very sensitive to the shape of the surface. The IOS and QC methods are not accurate in this region. Between 50 and 100 cm^{-1}, the cross sections are still quite sensitive to changes in the potential energy surface. Differences of over 50% are observed for some

transitions simply because of orbital basis set changes, holding all other levels of the calculations constant (see table 4, $j'=4$, DZ-CISDQ). Differences in the cross sections between the IOS and close coupling methods tend to be smaller than the differences that are due to the change in orbital basis sets for the potential energy surface.

Acknowledgments

REFERENCES

[1]   For an overview and references, see E.Herbst and W.Klemperer,
      Physics Today 29 (1976) 32,   and   W.D.Watson, Ann. Rev. Astron.
      Astrophys. 16 (1978) 585.

[2]   W.P.Kraemer and G.H.F.Diercksen, Astrophys. J. 205 (1976) L97.

[3]   B.J.Garrison, W.A.Lester,Jr., and H.F.Schaefer, J. Chem. Phys. 63
      (1975) 1449.

[4]   W.P.Kraemer and G.H.F.Diercksen, to be published.

[5]   S.Green and P.Thaddeus, Astrophys. J. 205 (1976) 766.

[6]   S.-I.Chu and A.Dalgarno, Proc. Roy. Soc. London A342 (1975) 191.

[7]   R.K.Nesbet, Advan. Quant. Chem. 9 (1975) 215.

[8]   C.E.Moore, Natl. Bur. Std. (U.S.) Circ. 467 (1949).

[9]   H.H.Landoldt and R.Bornstein, Zahlenwerte und Funktionen, Vol. 1
      (Springer, Berlin, 1951), part 3, p.511.

[10] G.Herzberg, Spectra of Diatomic Molecules (Van Nostrand, Princeton,
      1950).

[11] C.A.Burrus, J. Chem. Phys. 28 (1958) 427.

[12] D.E.Stogryn and A.P.Stogryn, Mol. Phys. 11 (1966) 371.

[13] L.D.Thomas, W.P.Kraemer and G.H.F.Diercksen, Chem. Phys. 30
      (1978) 33.

[14] L.D.Thomas, J. Chem. Phys. 67 (1977) 5224.

[15] M.Keil, J.T.Slankas and A.Kuppermann, J. Chem. Phys. 70 (1979) 541.

[16] A.D.Buckingham, Advan. Chem. Phys. 44 (1966) 4195.

[17] Extensive references to the IOS literature may be found in
      R.Goldflam, S.Green and D.J.Kouri, J. Chem. Phys. 67 (1977) 4149
      and R.Schinke and P.McGuire, Chem. Phys. 28 (1978) 129.

[18] R.N.Porter and L.M.Raff, in Dynamics of Molecular Collisions,

      ed. W.H.Miller (Plenum, New York, 1976), part B.

[19] S.Green, National Resource for Computation in Chemistry Software

      Catalogue, Vol. 1 (Lawrence Berkeley Laboratory, Berkeley, CA, 1980),

      Program No. KQ01 (MOLSCAT).

FIGURE CAPTIONS

Fig. 1.   Comparison of the V_λ term for the surfaces DZ-SCF (1), DZ-CISD (2),

DZ-CISDQ (3), TZ-CISDQ (4), and Green and Thaddeus (GT).

Fig. 2.   Comparison of the V_0 term inferred from experiment (EXPT) with

the theoretical V_0 terms (same notation as fig. 1).

Fig. 3. $V(R,\theta)$ vs. θ. $R = 5.0$ bohr for surfaces 1, 2, 3 and 4, and

$R = 4.67$ for the GT surface (same notation as fig. 1).

Fig. 4.   Comparison of $\log_{10}|V_\lambda|$ for V_0 from the TZ-CISDQ surface with

the asymptotic form $V_0 = -9.005 R^{-6}$ and for V_2 from the TZ-CISDQ

surface with the asymptotic form $V_2 = -1.503 R^{-6}$. Note that the

TZ-CISDQ V_λ terms converged very near the asymptotic forms for

$R \geqslant 12$.

Fig. 5.   Converged close-coupling, integral cross sections for the

surfaces 1, 3, 4 and GT (same notation as fig. 1).

Fig. 6.   Comparison of the close-coupling (CC) with the IOS and

quasiclassical (QC) cross sections computed with the

TZ-CISDQ surface.

TABLE 1. Computed interaction energies, $V(R,\theta)$ (atomic units), for the TZ-CISDQ, DZ-CISDQ, DZ-CISD, and DZ-SCF surfaces, where $V(R,\theta) = E(R,\theta) - E_\infty$.

R/θ	0.	45.0	70.0	90.0	110.0	135.0	180.0
TZ-CISDQ	$E_\infty = -116.02282444$						
3.0	.59325802	.15838764	.08059331	.06951884	.08510562	.14917124	.33402625
4.0	.12799430	.03892464	.01446531	.00990898	--	.02029978	.04253855
5.0	.02166042	.00675971	.00199319	.00104691	.00113490	.00211403	.00456331
6.0	.00307248	.00085024	.00012688	-.00001538	--	.00005788	.00028866
7.0	.00029408	.00002254	-.00005740	-.00006826	-.00006689	-.00007124	-.00006634
8.0	-.00003769	-.00004850	-.00004556	-.00004052	-.00003770	-.00004236	-.00004985
9.0	-.00004795	-.00003364	-.00002412	-.00001966	-.00001877	-.00002073	-.00002519
10.0	-.00002531	-.00001691	-.00001154	-.00000909	-.00000863	-.00000976	-.00001154
11.0	-.00001178	-.00000773	-.00000545	-.00000482	-.00000484	-.00000505	-.00000600
12.0	-.00000506	-.00000399	-.00000333	-.00000306	-.00000285	-.00000274	-.00000314
DZ-CISDQ	$E_\infty = -115.97422138$						
3.0	.64036688	.16124677	.08181858	.07015504	.08575504	.15073336	.33628936
4.0	.12871457	.03988763	.01506937	.01029869	.01176767	.02069882	.04337528
5.0	.02230362	.00723413	.00231835	.00128151	.00132892	.00227390	.00473631
6.0	.00333174	.00104259	.00021656	.00004800	.00005338	.00014972	.00035890
7.0	.00037648	.00007750	-.00005612	-.00007556	-.00006581	-.00005203	-.00004470
8.0	.00000264	-.00003587	-.00005533	-.00005219	-.00004634	-.00004566	-.00005160
9.0	-.00002994	-.00003454	-.00003167	-.00002628	-.00002348	-.00002406	-.00002782
10.0	-.00002961	-.00002282	-.00001708	-.00001341	-.00001159	-.00001156	-.00001321
11.0	-.00001832	-.00001375	-.00000963	-.00000707	-.00000587	-.00000573	-.00000595
12.0	-.00001102	-.00000784	-.00000521	-.00000393	-.00000341	-.00000292	-.00000308
DZ-CISD	$E_\infty = -115.94670388$						
3.0	.60794997	.16078197	.08173503	.07067738	.08669786	.15194810	.33707947
4.0	.13076234	.03995547	.01507956	.01041492	.01194075	.02086512	.04334588
5.0	.02260153	.00725260	.00233020	.00131454	.00137116	.00231381	.00473494
6.0	.00338178	.00105379	.00022925	.00006302	.00006957	.00016551	.00037211
7.0	.00039384	.00008602	-.00004730	-.00006688	-.00005727	-.00004298	-.00003426
8.0	.00001028	-.00003046	-.00005019	-.00004766	-.00004207	-.00004076	-.00004555
9.0	-.00002578	-.00003097	-.00002885	-.00002408	-.00002147	-.00002183	-.00002508
10.0	-.00002397	-.00002057	-.00001553	-.00001221	-.00001057	-.00001056	-.00001199
11.0	-.00001646	-.00001244	-.00000873	-.00000644	-.00000535	-.00000520	-.00000542
12.0	-.00000997	-.00000712	-.00000476	-.00000358	-.00000307	-.00000264	-.00000277

TABLE 1 (continued)

R/θ	0.	45.0	70.0	90.0	110.0	135.0	180.0
	DZ–SCF	E_∞ = –115.63100362					
3.0	.64482488	.16134136	.08273624	.07393895	.09239170	.15988849	.34492680
4.0	.13986061	.04134128	.01576503	.01141077	.01326915	.02240027	.04438636
5.0	.02440692	.00772205	.00259497	.00161926	.00173420	.00272263	.00508052
6.0	.00381744	.00122980	.00035649	.00018337	.00019540	.00030106	.00052890
7.0	.00054739	.00016597	.00002046	–.00000523	.00000259	.00002232	.00004688
8.0	.00006883	.00001013	–.00001410	–.00001655	–.00001296	–.00000762	–.00000346
9.0	.00000227	–.00000699	–.00000989	–.00000924	–.00000813	–.00000708	–.00000647
10.0	–.00000544	–.00000616	–.00000552	–.00000463	–.00000414	–.00000409	–.00000411
11.0	–.00000485	–.00000433	–.00000333	–.00000258	–.00000209	–.00000192	–.00000194
12.0	–.00000356	–.00000285	–.00000204	–.00000149	–.00000109	–.00000086	–.00000079

TABLE 2. Parameters for the analytic fits, Eq. (2), to the energies in Table 1.

λ	0	1	2	3	4	5	6
TZ-CISDQ							
a_1	37.9768	36.6203	62.5331	22.6280	45.2342	65.5859	205.118
a_2	-11.7923	-8.76206	-24.3656	-7.38362	4.97911	-12.4564	-47.5238
a_3	3.06004	2.72019	7.52403	1.99509	0.652702	3.79673	12.4003
a_4	-0.575762	-0.525131	-1.51857	-0.349623	-0.177533	-0.563704	-1.62025
a_5	0.065529	0.069589	0.193626	0.036989	0.023365	0.058920	0.174795
b_1	1.55556	1.55309	1.48395	1.47037	2.08272	2.11728	2.45185
b_2	1.24444	1.24247	1.18716	1.17630	1.66617	1.69383	1.96148
b_3	0.995556	0.993975	0.949728	0.941037	1.33294	1.35506	1.56919
b_4	0.796444	0.795180	0.759783	0.752830	1.06635	1.08405	1.25535
b_5	0.637156	0.636144	0.607826	0.602264	0.853080	0.867240	1.00438
c_1	-29.5779	-433.277	-105.355	-183.514	-231.362	-355.896	-378.169
m_1	6	7	6	7	8	8	8
DZ-CISDQ							
a_1	264.495	142.274	494.375	101.274	126.190	59.5901	14.2223
a_2	-514.313	-279.371	-910.791	-187.122	-217.750	-105.619	-27.9310
a_3	-345.545	188.985	580.227	118.847	128.573	63.9121	18.6458
a_4	-80.1167	-43.9144	-127.249	-25.8562	-25.9194	-13.1904	-4.22902
b_1	1.22278	1.13172	1.33559	1.18676	1.31027	1.29061	1.05338
b_2	1.16162	1.07513	1.26881	1.12742	1.24476	1.22608	1.00071
b_3	1.10354	1.02138	1.20537	1.07105	1.18252	1.16478	0.950672
b_4	1.04836	0.970306	1.14510	1.01749	1.12340	1.10654	0.903138
DZ-CISD							
a_1	263.031	140.198	499.728	106.082	132.511	64.1102	14.7549
a_2	-508.791	-273.866	-915.208	-194.550	-227.679	-110.826	-28.5239
a_3	340.149	184.273	579.868	122.688	133.913	65.4022	18.7565
a_4	-78.4953	-42.5902	-126.514	-26.5094	-26.8976	-13.1608	-4.19323
b_1	1.22939	1.13231	1.34518	1.19845	1.32048	1.32495	1.08101
b_2	1.16792	1.07570	1.27792	1.13852	1.25446	1.25870	1.02696
b_3	1.10952	1.02191	1.21402	1.08160	1.19174	1.19577	0.975611
b_4	1.05404	0.970816	1.15332	1.02752	1.13215	1.13598	0.926830

(continued . . .)

TABLE 2 (continued).

| λ	0	1	2	3	4	5	6
DZ-SCF							
a_1	234.695	109.717	418.386	89.7842	133.216	49.8396	7.27046
a_2	-431.989	-208.489	-709.770	-147.694	-212.352	-64.5695	-2.59914
a_3	275.105	135.964	421.024	83.9215	116.516	28.8211	-3.17015
a_4	-60.4954	-30.3691	-86.5705	-16.3998	-21.9028	-4.38090	1.39877
b_1	1.26912	1.09893	1.42698	1.27564	1.41050	1.60000	1.53856
b_2	1.20566	1.04399	1.35563	1.21186	1.33998	1.52000	1.46163
b_3	1.14538	0.991787	1.28785	1.15127	1.27298	1.44400	1.38855
b_4	1.08811	0.942198	1.22345	1.09371	1.20933	1.37180	1.31912

TABLE 3. Percent difference between the analytic fit and computed
energies for the TZ-CISDQ surface.

| R/θ	0.	45.0	70.0	90.0	110.0	135.0	180.0
3.0	-0.6	-1.1	-1.3	-2.0	-2.4	-1.5	-0.5
4.0	-0.1	0.7	3.0	4.3	——	4.1	4.2
5.0	0.8	2.4	5.2	2.6	-3.5	-3.1	-1.8
6.0	-0.3	0.1	-0.8	53.7	——	-25.9	-1.6
7.0	-2.7	-5.2	-2.8	-1.1	0.9	-1.5	-10.7
8.0	1.7	0.1	0.0	1.1	1.4	1.4	-1.3
9.0	3.4	2.1	1.6	1.8	4.2	2.3	2.5
10.0	-3.3	-1.4	0.2	-2.1	-4.4	-2.6	-3.7
11.0	-1.2	-3.8	-5.6	0.4	1.0	1.1	2.2
12.0	7.1	10.0	6.0	11.3	7.1	8.3	3.4

TABLE 4. Percent differences between the close-coupling cross sections for the TZ-CISDQ surface and all other cross sections. Under GT, DZ-SCF and DZ-CISDQ are the percent differences for the close-coupling results on those surfaces. Under IOS and QC are the differences for those approximations on the TZ-CISDQ surface. The differences are for the rotational transitions $0 \to j'$

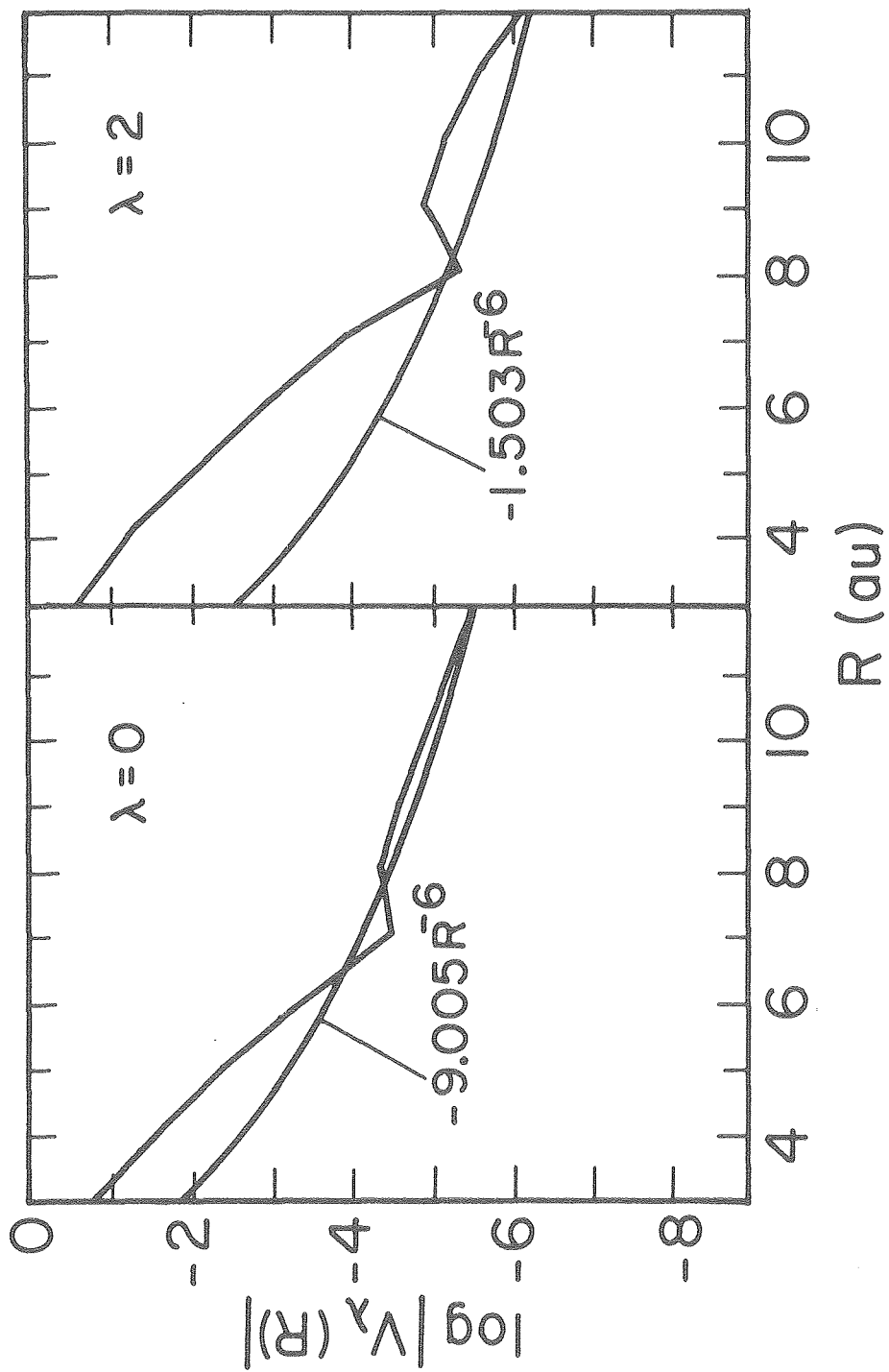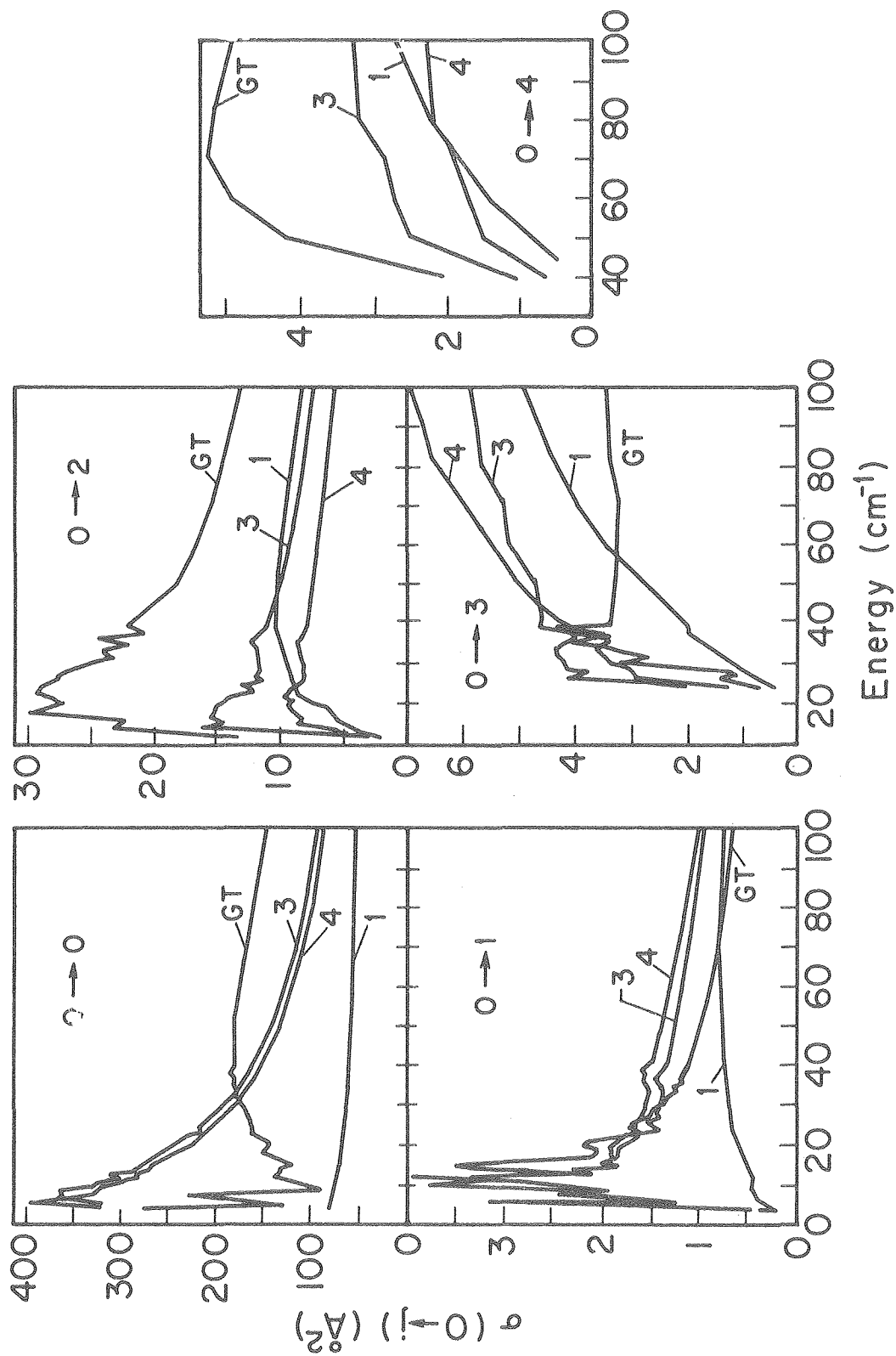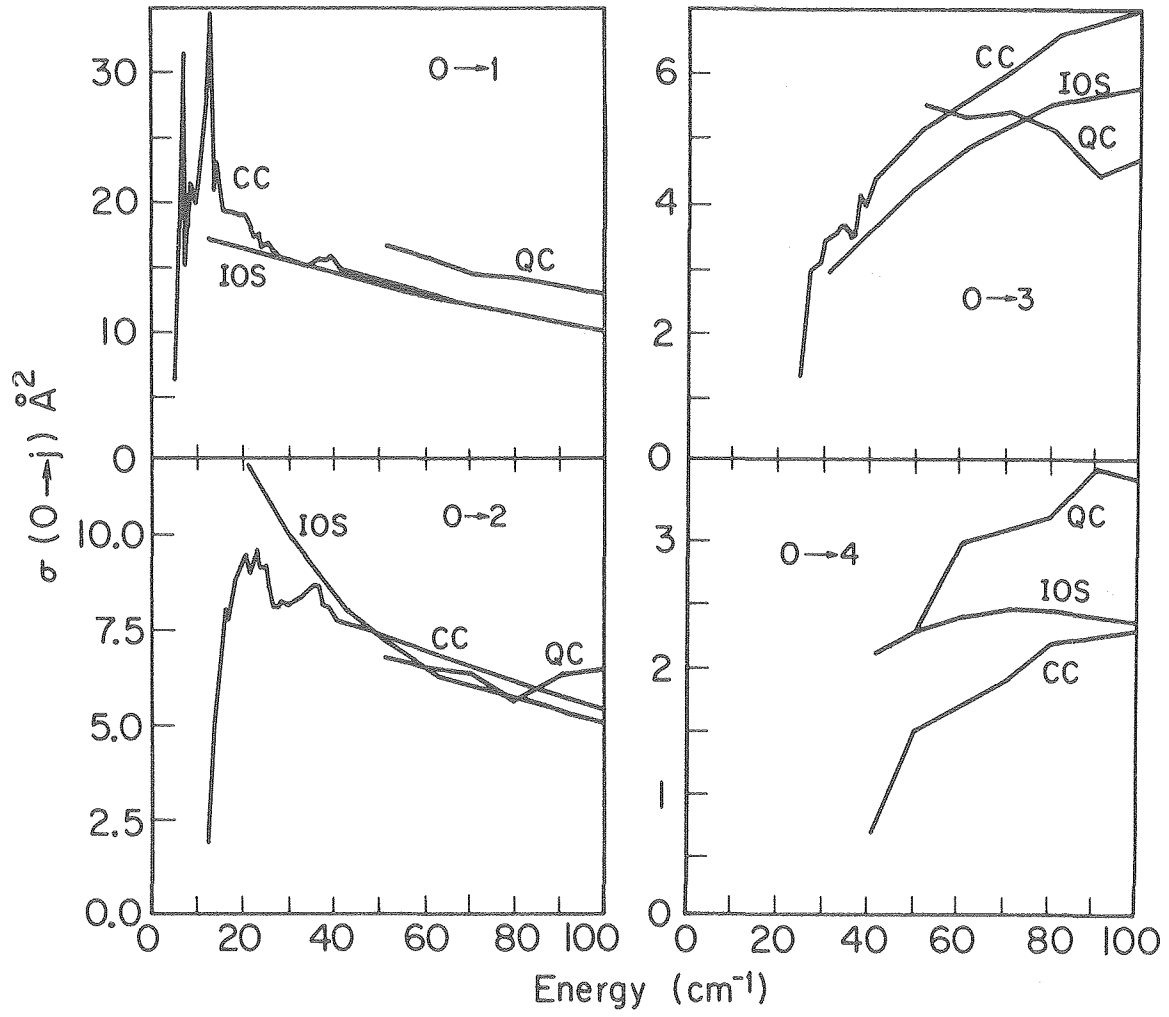| j'	E (cm^{-1})	GT	DZ-SCF	DZ-CISDQ	IOS	QC
0	50	37	−56	7	0	—
	70	57	−48	8	0	—
	80	63	−44	8	0	—
	100	70	−38	8	0	—
1	50	−29	—	−10	−3	20
	70	−34	−34	−8	−1	20
	80	−34	−31	−8	0	24
	100	−34	−25	−5	0	27
2	50	147	39	35	−1	−8
	70	133	42	30	−4	−7
	80	135	45	30	−7	−7
	100	132	45	28	−9	17
3	50	−36	−45	−6	−16	8
	70	−46	−33	−12	−14	−11
	80	−48	−33	−13	−16	−22
	100	−50	−29	−15	−17	−33
4	50	182	−45	69	53	53
	70	178	−4	51	30	63
	80	139	1	48	13	46
	100	117	19	44	3	53
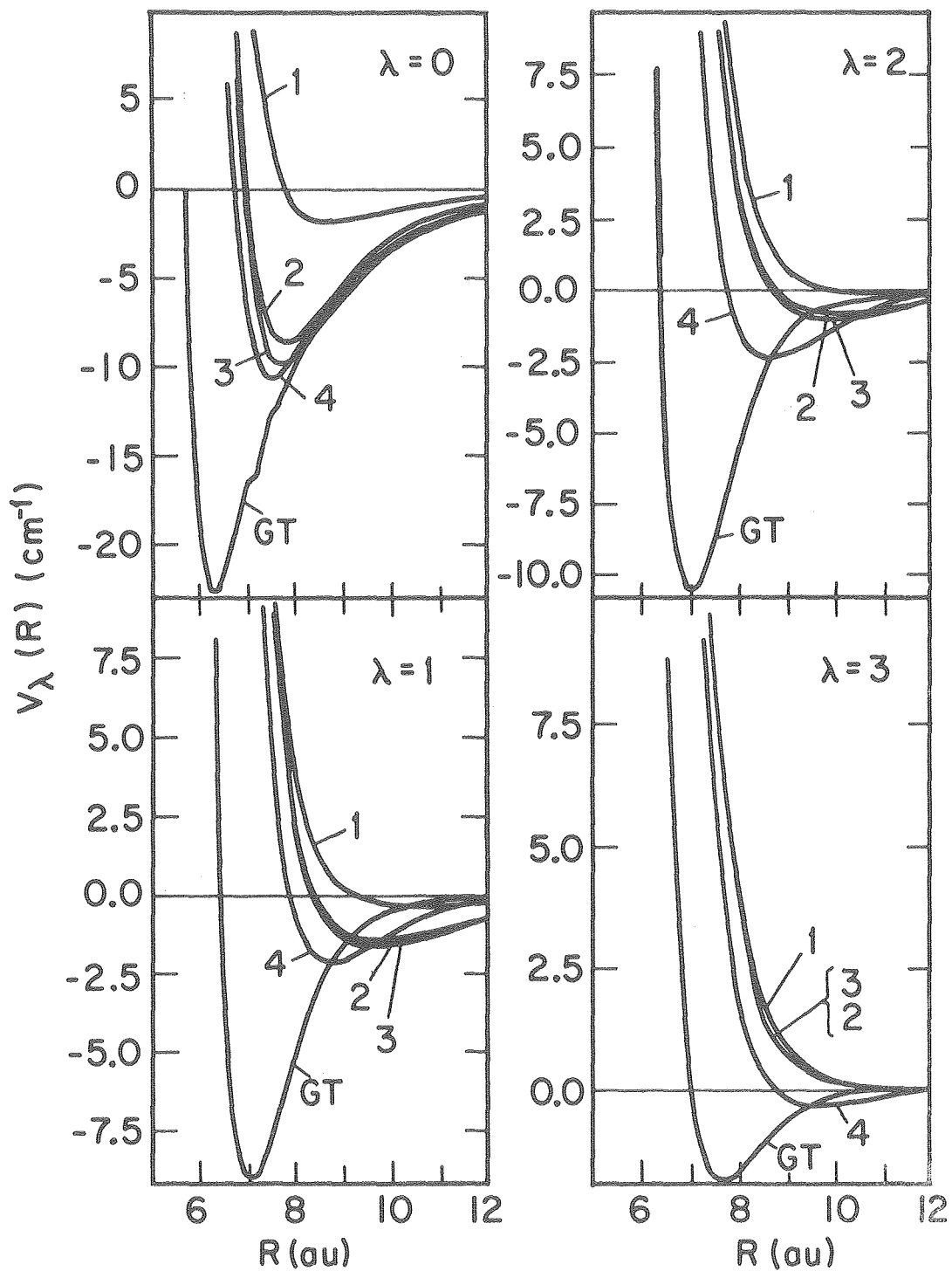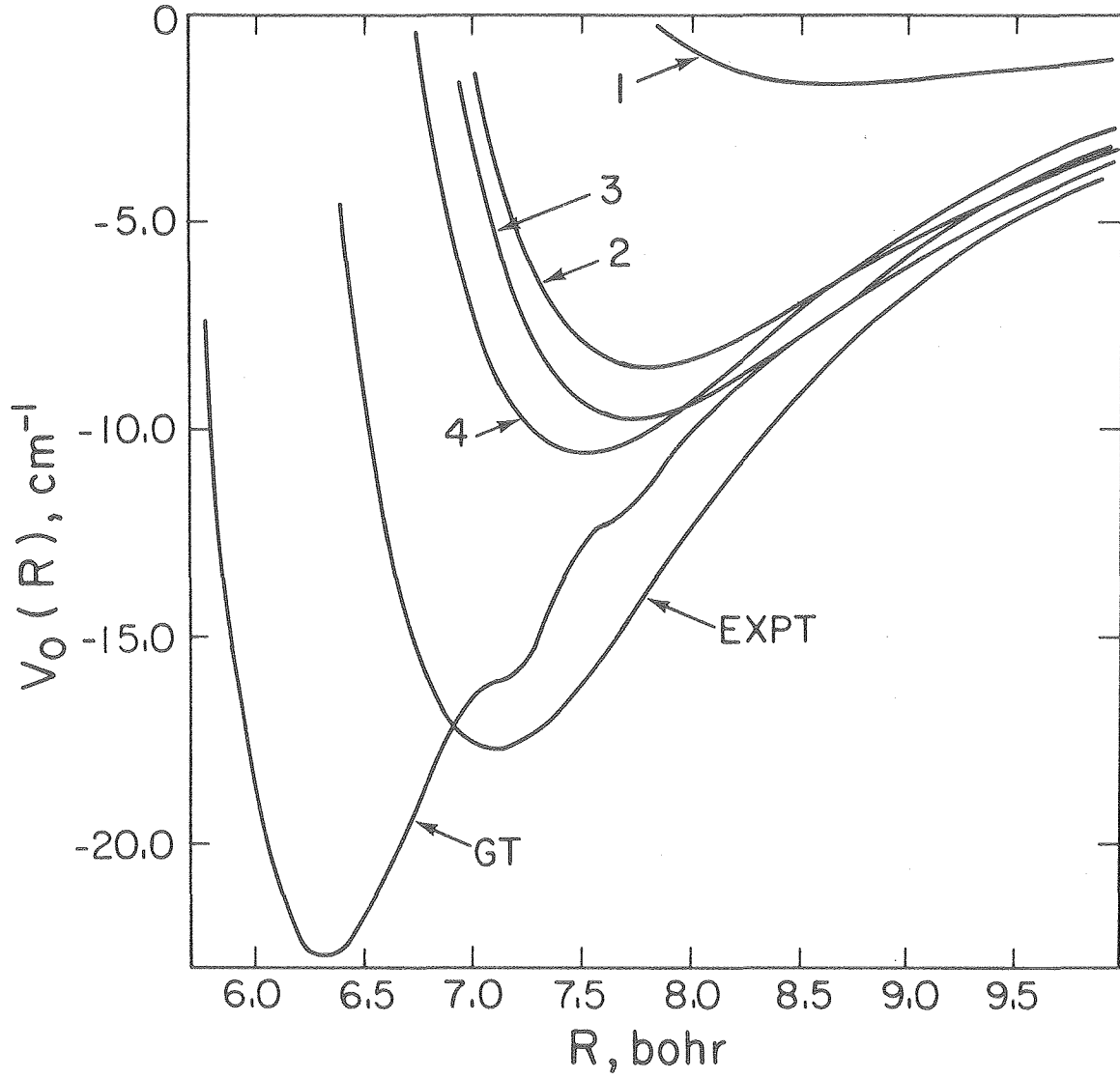
XBL7910-3830

XBL 804-604
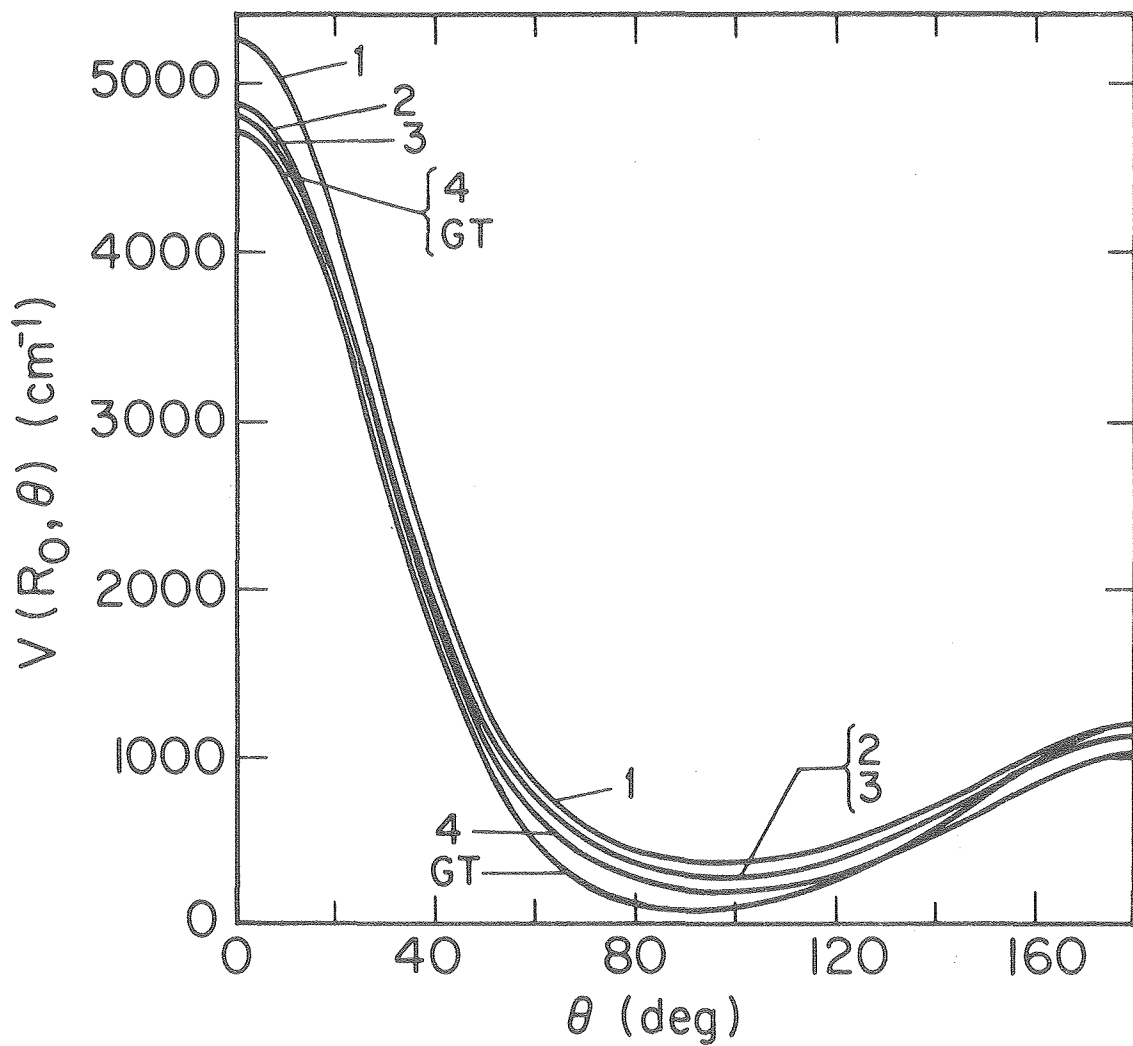
XBL7910-3829

XBL7910−3828

XBL79IO-3831

XBL7910-3832